ISSN (Print): 2476-8316
ISSN (Online): 2635-3490
Dutse Journal of Pure and Applied Sciences (DUJOPAS), *Vol. 4 No. 2 December 2018*

First-Principles Calculations of Optoelectronic Properties of Bi_2se_3 Surface State for Broadband Photodetector

[1]Abdullahi Lawal *, [2]A. B.Suleiman, [3]A. S Gidado
[1]Department of Physics, Federal College of Education Zaria,
P.M.B 1041 Zaria, Nigeria
Email: abdullahikubau@yahoo.com
[2]Department of Physics, Federal University,
Dutse, Jigawa State, Nigeria
[3]Department of Physics, Bayero University
Kano, PMB 3011 Kano, Nigeria

Abstract
It has been established experimentally that bismuth selenide (Bi_2Se_3) is van der Waals layered materials of technological importance, with metallic surface state. Formation of a single Dirac cone similar to graphene inside the bulk band gap energy by the surface state is a key requirement toqualifyBi_2Se_3 for future optoelectronic applications. Therefore, to expose its hidden potentials, detailed analysis of the electronic and optical properties of its surface sate at the level of more efficient and reliable techniques is very essential. To accomplish this purpose, we investigated the electronic and optical properties of the surface states using the recently developed Cooper's exchange potentials (vdW-DF^{C09}x) within Density Functional Theory (DFT) framework. Our surface states band structure calculations with the inclusion of vdW-DF^{C09}x functionals reveals that Bi_2Se_3 has energy gap 0.700, 0.221, 0.116 and 0.065 eV at Γ pointfor 1QL, 2QL, 3QL and 4QL films respectively. These values are in good agreement with experimental measurement. The results of optical absorption show that Bi_2Se_3 surface state has strong absorption in the near infrared to ultraviolet wavelenghts, therefore, it can be used in optoelectronics applications such asoptical communication, biomedical imaging, motion detector, remote sensing, and gas sensing.

Keywords: Sb_2Te_3, Graphene, Photodetector, vdW-DF^{C09}x, DF

INTRODUCTION
Although optoelectronic technology is growing, the need of high-performance broadband photodetector that can detect light from ultraviolet to infrared frequency is becoming more eminent(Yao et al., 2015, Lawal et al., 2017, Mahdi et al., 2018).Though, many efforts were done on transition metal oxides (TMOs) and transition metal dichalcogenides (TMDCs) for this intention, energy band gap of 1.0 to 3.3 eV has limited their application for the detection of light in the near-infrared region (Zhang et al., 2014).In order to cope with these issues,second generation topological insulator (2GTI) mainly Sb_2Te_3, Bi_2Te_3 and Bi_2Se_3, would be a better choice (Qiao et al., 2015, Kim et al., 2016, Kim et al., 2017, Wang et al., 2017).These compounds are layered materials of technological significance with someunique characteristics such as: extremely simple surface state, small band gap, protected conducting surface states, single Dirac cone at the surface, saturable absorber behaviour, low saturable optical intensity, large modulation depth, high damage threshold and low cost (Lee et al., 2015, Hasan and Kane, 2010). Their topological naturestrongly depends on relativistic spin-orbit coupling (SOC) and protected by time-reversal symmetry.Also, these materials are spin-momentum locked due to the presence of strong SOC and their spin polarization is

**Author for Correspondence*

determined with respect to the direction of their motion. The three dimension (3D) 2GTI have narrow band gap in the mid-infrared wavelengths region in the range between 0.15 to 0.35 eV while two dimension (2D) show metallic surface states at all interface with a dielectric such as vacuum. Furthermore, the 2D energy dispersion relation near the Fermi level of the conducting states is linear, showing a single Dirac cone of massless particle similar to graphene. However, this exotic metallic state renders these novel materials suitable for applications, particularly optoelectronics, spintronics and plasmonics. It is also well known that these compoundsbelong to rhombohedral crystal structure with (R-3m) space group containing five atoms per unit cell. In therhombohedral crystal structure there are three Te atoms differentiated by two atoms as Te-1 and Te-2 respectively while Bi and Sb atoms are equivalent.(Chen et al., 2010, Liu et al., 2010, Zhang et al., 2009a). Alternatively three rhombohedral crystal structures form hexagonal structure. It is clear within hexagonal crystal structure that 2GTI are layered compounds in the form of slab with five atomic layer regards as quintuple-layer (QL).The hexagonal crystal structures of Bi_2Se_3 is showed in Figure 1.Among these, Bi_2Se_3 have received extensive attention as an appealing candidate for converting light into electrical signals, because of its direct energy gap in 3D, simple metallicDirac surface state, strong light absorption, high photoconversion efficiencies, low cost, and so on (Yue et al., 2018, Li et al., 2018, Das et al., 2017).Therefore, for a better understanding of its optoelectronic behavior in 2D, detailed knowledge of theelectronic and optical properties ofBi_2Se_3 surface states at the level of more efficient and reliable techniques is essential to expose its hidden potential fordevice applications such as photo-detectors.It has been established that first-principles many-body calculations would be suitable with fully self-consistent GW, because it provides true quasiparticle energies (Hybertsen and Louie, 1986). However, both self-consistent and nonself-consistent GW approaches are computationallyprohibited for surfacescalculations of 2GTIs (Crowley et al., 2015). On the other hand, it is generally accepted that first-principles calculations based onlocal density approximation (LDA) and generalised gradient approximation of PBE (Perdew et al., 1996)are practical for surface states calculations(Crowley et al., 2015, Popov et al., 2014, McIver et al., 2012, Zhang et al., 2009a, Zhang, 2015).To the best of our knowledge, surface states electronic band structure and optical properties calculations withCooper's exchange functionals (vdW-DF^{C90}x) on Bi_2Se_3 have not beenreported yet.

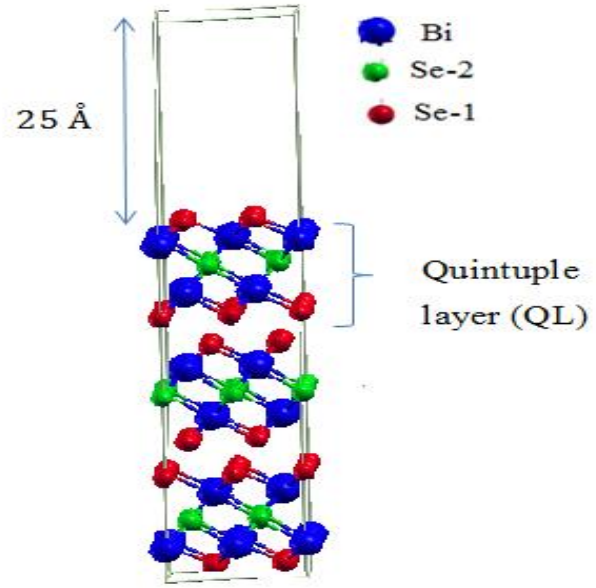

Fig. 1:(a) Crystallographic geometry of Bi_2Se_3

THEORETICAL METHODOLOGY

In this paper, the calculation is performed based on plane wave basis set ground-state DFT code, called Quantum Espresso (Giannozzi et al., 2009). Full relativistic norm-conserving pseudopotentials generated using Rappe-Rabe-Kaxiras-Joannopoulos (RRKJ) technique were used to model the interactions between the valence electrons and ionic core potential of Bi, Se-1, and Se-2atoms with the inclusion of spin-orbit coupling (SOC). An electron orbital of $6s^2\ 6p^3\ 5d^{10}$ and $4s^2\ 4p^4$ for Bi and Se were used as valence electrons throughout the calculations. The surface state band structure calculations of Sb_2Te_3 have been performed within 1 to 4 quintuples (QLs) slabs. In addition to the semi-local PBE, we implemented the recently developed Coope's exchange functionals (vdW-DF^{C09}x) to take into account the effect of van der Waals (vdW) interaction. To avoid unwanted interactions between the nearest slabs, a large vacuum layer of 25Å was used so that periodic images and the layer can be treated independently as can be seen in Fig. 1. A 11×11×1 k-point mesh grid was used for the integration of the Brillouin zone (BZ). Plane-wave basis set with kinetic energy cut-offs of 80 Ry was used to expand the electron wave functions and 450 Ry for charge density. Also, the atomic positions,size andshape of the supercell slab geometry are relaxed until Hellmann-Feynman forces acting on each ion becomeless than10^{-3} eV/Å. This method is adopted in this work because the thickness at which the massless Dirac cone forms for this compound is difficult to be observed experimentally even with angle-resolved photoemission spectroscopy (Crowley et al., 2015). The selected high symmetry points are $K\left(\frac{1}{3},\frac{2}{3},0\right)$, Γ(0,0,0) and $M\left(0,\frac{1}{2},0\right)$ respectively. For optical properties calculations

To complete the study on the optoelectronic properties in addition to electronic band structure, comprehensive investigations are presented on the optical properties of the above-said compound using Coope's exchange (vdW-DF^{C09}x). The study of optical properties due to electronic transition is related to electronic properties. Transitions between occupied and unoccupied states are caused by the electric field of the photon. However, when performing calculations on optical properties, the complex dielectric constant is evaluated, and the other properties are expressed in terms of it. The complex dielectric constant ε is given by $\varepsilon(\omega) = \varepsilon_1(\omega) + i\varepsilon_2(\omega)$, where ε_1 and ε_2 are real and imaginary parts of dielectric constant respectively. Thus, the complex dielectric function is suitable to describe the optical properties at microscopic level or quantum mechanical level. The expression for the complex imaginary part of dielectric function $\varepsilon_2(\omega)$ has been derived in equation 1. Using $\varepsilon_2(\omega)$, $\varepsilon_1(\omega)$ is obtained using the Kramer–Kronig transformation (Lucarini et al., 2005) as given in relation (2) in the following.

$$\varepsilon_2(\omega) = \frac{2\pi e^2}{\Omega\varepsilon_0}|\langle\psi_k^c|\hat{u}\times\vec{r}|\psi_k^v\rangle|\delta\left(E_k^c - (E_k^v + E)\right) \quad (1)$$

$$\varepsilon_1(\omega) = 1 + \left(\frac{2}{\pi}\right)\int_0^\infty d\omega' \frac{\omega'^2\varepsilon_2(\omega')}{\omega'^2 - \omega^2} \quad (2)$$

where P is the principal value of the integral and the integral is over the irreducible Brillouin zone. With the knowledge of real and imaginary parts of dielectric function then other optical parameters can be obtained as follows.

$$\alpha(\omega) = \frac{\omega}{c}\sqrt{2\left(\sqrt{\varepsilon_1^2(\omega) + \varepsilon_2^2(\omega)} - \varepsilon_1(\omega)\right)} \quad (3)$$

$$L(\omega) = \frac{\varepsilon_2(\omega)}{\varepsilon_2(\omega) + \varepsilon_1(\omega)} \quad (4)$$

RESULTS AND DISCUSSION

Electronic Properties

Electronic band structure calculations are very important for describing the optoelectronicbehaviour of any materials. However, due to the limitation of computational resources, thin film calculations of Sb_2Te_3, Bi_2Se_3 and Bi_2Te_3 with more than 4 quintuple layers (QLs) are not performed in this work, because as slab thickness increases the time cost for the first-principles calculations also increases very rapidly. The calculated band dispersions of Bi_2Se_3 slabs with thickness from 1QL to 4QL along special symmetry directions of the irreducible Brillouin zone setting Fermi energy level scale at 0 eV are presented in Fig. 2. In Bi_2Se_3 surface states, the most important properties is the formation of single Dirac cone in the band structure at the Γ point (Yazyev et al., 2010, Liu et al., 2010, Sarkar et al., 2018, Boulares et al., 2018). For full first-principles approach, we fully relaxed the slab structures using vdW-DF^{C09}x corrections.. The calculated band dispersions of Bi_2Se_3 slabs with thickness from 1QL to 4QL are presented in Fig.2. The 1QL, 2QL, 3QL and 4QL films shows an energy gap at Γ point of 0.700, 0.221, 0.116 and 0.065 eV and these values are in quite good agreement with experimental results (Zhang et al., 2009b). The presence of energy gap at Γ point for Bi_2Se_3 film up to 4QLs has been observed in prior experimental measurement (Zhang et al., 2009b).

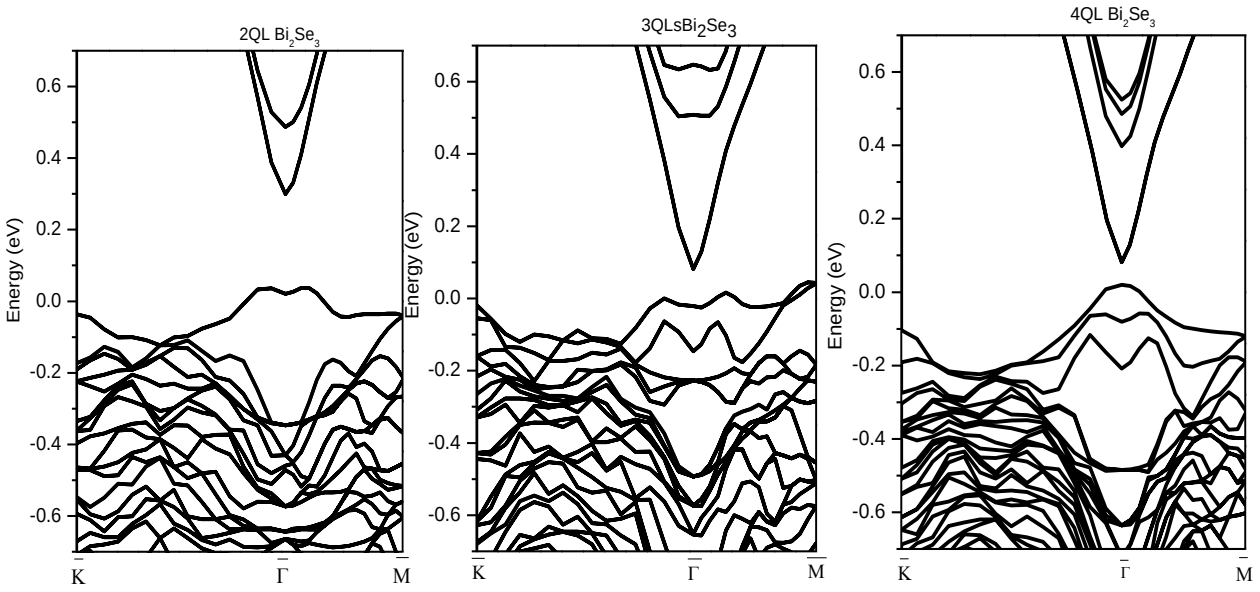

Fig. 2: Band structures of Bi_2Se_3 films with 2 QL, 3 QL and 4 QL

Also, the conduction bands for each of the film band structures are parabolic and located at Γ point as can be seen in Fig. 2. The conduction band at the Γ point of 1 QL band structure is composed of 39% Bi p_{xy}, 16% Bi p_{xy}, 13% Se s, and 24% Se p_{xy}.The orbital composition of the Γ valley for Bi_2Se_3 film from one up to four quintuple layers remains the same. Fig.3 presents the results of the energy gap at Γ point as a function of the film thickness of Bi_2Se_3 along with experimental and previous GW results. Our results pointed out that standard DFT band structures calculation within PBE+vdW-DF^{C09}x is able to give accurate qualitative prediction of the topologically nontrivial electronic structure of Bi_2Se_3 than GW approach. The plots of energy gap at Γpoint as a function of the film thickness of Bi_2Se_3 show that the results obtained within GW approximations by Yazyev et al. (Yazyev et al., 2012) are somehow larger than experimental values (Zhang et al., 2009b).

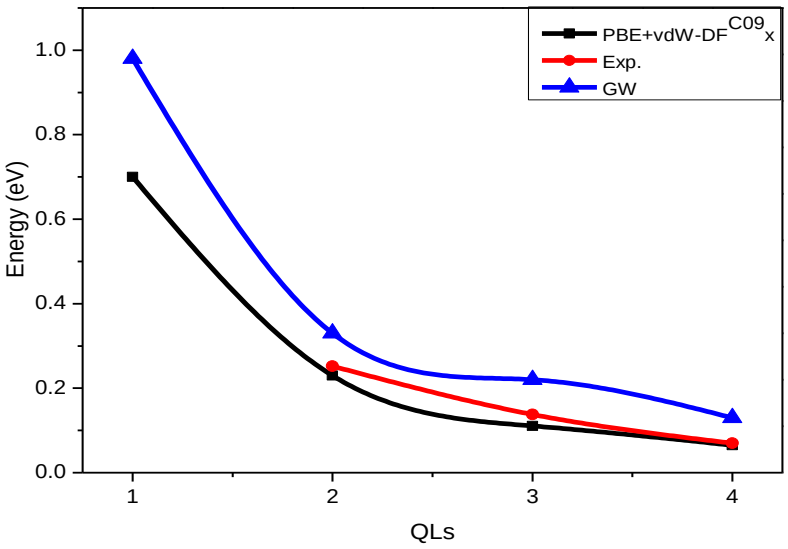

Fig. 3: Energy gap in function of film thickness for Bi_2Se3

Optical Properties

Optical properties of a material explain the behaviour of material when exposed to electromagnetic radiations (Lawal et al., 2018, Lawal et al., 2017). From the literature review, it was found that the exploration of the optical properties of Bi_2Se_3surface state is scarcely done.The imaginary part of themacroscopic dielectric function is a quantity that provides useful information on how much material is capable to absorb photon energy while the real part describes how much material becomes polarized as a result of induced electric dipole creation when theexternal electric field is applied.Fig. 4(a) shows the graph of absorption spectrum $\varepsilon_2(\omega)$ of Bi_2Se_3as a function of energy. The calculated optical absorption with polarization along x-direction (in-plane)shows that the first critical point (optical absorption edged)occurred at 0.064 eV with strong absorption in the energy range from 0.9 to 9.6 eV. These values indicated that the material under investigation can absorb light within wide energy range from near infrared spectra to ultraviolet region. On the other hand, the graph ofoptical absorption confirmed that Bi_2Se_3thin film lead to the increase in optical absorption when compared to the bulk form ofBi_2Se_3as can be seen in our previous work(Lawal et al., 2017). Since Bi_2Se_3exhibit good absorption in the near infrared to ultraviolet range, therefore, it can be used in optoelectronics applications such as laser photonic, optical communication, biomedical imaging, remote sensing, solar cell and gas sensing.Fig. 4(b) shows the calculated real part of thedielectric functionin the energy range from 0 to 28 eV. The value of the dielectric constant $\varepsilon(\infty)$ was found to be 37.6. Also, the real part of the dielectric function $\varepsilon_1(\omega)$becomes negative from 6.5 eV, indicating that the material under investigation possesses plasmonicbehavior. The change of $\varepsilon_1(\omega)$from positive to negative at about 6.5 eV suggest that Bi_2Se_3 should starts resonating at energy greater than 6.5 eV.

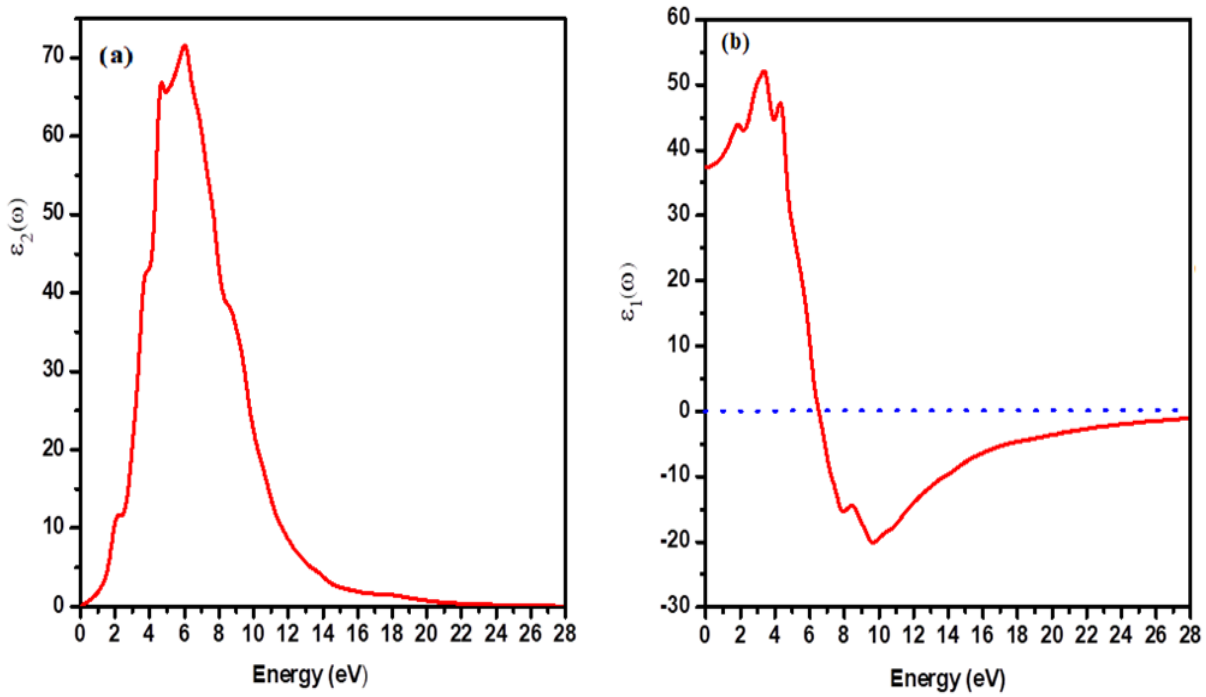

Fig. 4(a) imaginary part of the dielectric function (b) real part of the dielectric function of Bi_2Se_3 surface states calculated using vdW-DF^{C09}x.

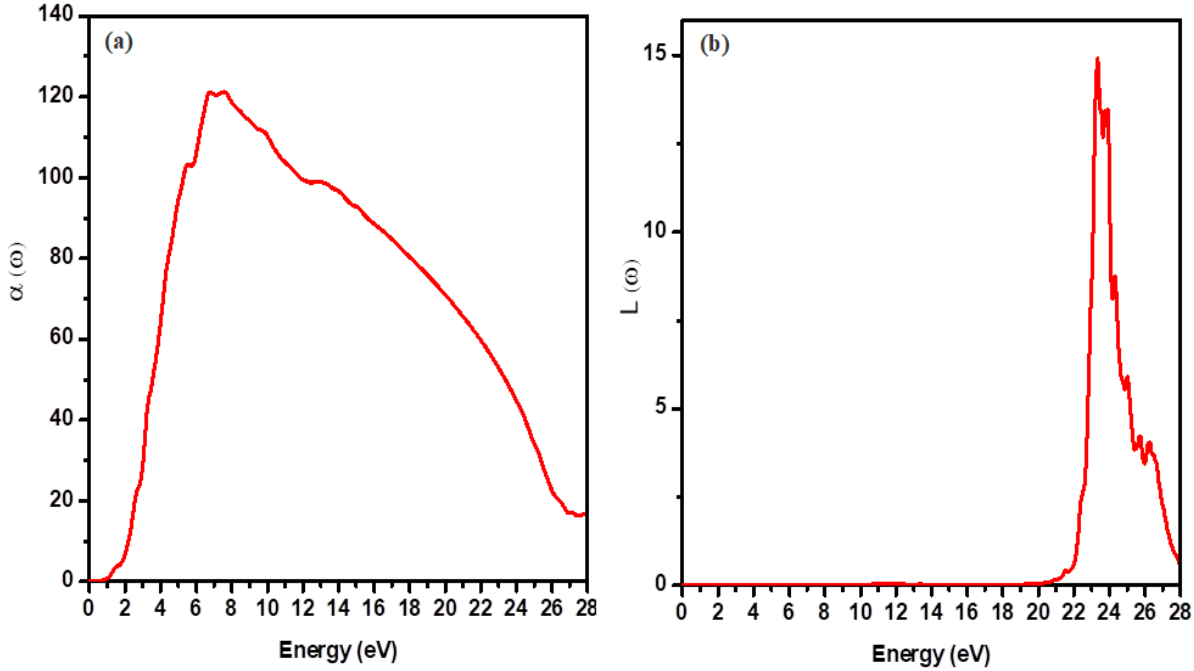

Fig. 5(a)Energy spectra of absorption coefficient $\alpha(\omega)$(b)EELs of Bi_2Se_3 surface states calculated using vdW-DF^{C09}x.

This plasmonic behaviour of Bi_2Se_3 is another exciting feature that qualifies it as a promising candidate for many applications (Savoia et al., 2015, Xiong et al., 2014, Rodríguez-Fortuño et al., 2014).Absorption coefficient $\alpha(\omega)$ is used to describe the extent to which a material absorbs photon energy. Absorption coefficient $\alpha(\omega)$ represented in Fig. 5(b) depicts that the absorption region is more stretched to higher energy. The variation of optical absorption indicates the prospective use of Bi_2Se_3 for device applications, which can be operated over a wider range of energy scale.The study of EELS$L(\omega)$ is an important factor as it describes

energy of fast moving electron that interact with a material and loses energy per unit length(Kittel et al., 1996). The graph of energy loss function is represented in Fig. 5 (b).Energy loss could be due to inelastic interactions, phonon excitations, inter and intra band transitions, and inner shell ionization. The feature behaviour of the prominent peaks in the spectra represents the characteristics of plasma resonance which is found to be 23.6 eV. This sharp maximum peak of the energy loss function spectra appears at a particular incident light frequency which corresponds to the trailing edges in the reflection spectra sometimes called plasma frequency ω_P. At this point of energy, the real part of the dielectric function goes to zero indicating rapid reduction in reflectance.The sharp maxima peak of the energy loss function spectra is related to an abrupt reduction in reflection spectra.

CONCLUSION

In summary, we have performed first-principles calculations of the electronic and optical properties of Bi_2Se_3 surface states using DFT pseudo potential approach within the most recently developed Cooper's exchange (vdW-DF^{C09}x).The band dispersions calculations of Bi_2Se_3films with Van der Waals interaction reveal that; at the thinner film, the strong interaction between the bottom surface and top surface bands resulted in an energy gap at Γ point and the magnitude of the gap decays rapidly by increasing the thickness of the film. Interestingly, the energy gapsfor 1QL, 2QL, 3QL and 4QL at Γ point were found to be 0.700, 0.221, 0.116 and 0.065 eV respectively at Γ point. The values of the band gap at Γ point are in agreement with the available experimental result as compared to the results obtained by the bare PBE and GW approaches.The results of optical parameter show that Bi_2Se_3 has strong absorption in the near infrared to ultraviolet wavelenghts, therefore, it can be used in optoelectronics application like laser photonic, optical communication, biomedical imaging, remote sensing, solar cell and gas sensing.

REFERENCES

BOULARES, I., SHI, G., KIOUPAKIS, E., LOŠŤÁK, P., UHER, C. & MERLIN, R. 2018. Surface phonons in the topological insulators Bi2Se3 and Bi2Te3. *Solid State Communications,* 271**,** 1-5.

CHEN, Y., CHU, J.-H., ANALYTIS, J., LIU, Z., IGARASHI, K., KUO, H.-H., QI, X., MO, S.-K., MOORE, R. & LU, D. 2010. Massive Dirac fermion on the surface of a magnetically doped topological insulator. *Science,* 329**,** 659-662.

CROWLEY, J. M., TAHIR-KHELI, J. & GODDARD III, W. A. 2015. Accurate Ab Initio Quantum Mechanics Simulations of Bi2Se3 and Bi2Te3 Topological Insulator Surfaces. *The journal of physical chemistry letters,* 6**,** 3792-3796.

DAS, B., DAS, N. S., SARKAR, S., CHATTERJEE, B. K. & CHATTOPADHYAY, K. K. 2017. Topological Insulator Bi2Se3/Si-Nanowire-Based p–n Junction Diode for High-Performance Near-Infrared Photodetector. *ACS applied materials & interfaces,* 9**,** 22788-22798.

GIANNOZZI, P., BARONI, S., BONINI, N., CALANDRA, M., CAR, R., CAVAZZONI, C., CERESOLI, D., CHIAROTTI, G. L., COCOCCIONI, M. & DABO, I. 2009. QUANTUM ESPRESSO: a modular and open-source software project for quantum simulations of materials. *Journal of physics: Condensed matter,* 21**,** 395502.

HASAN, M. Z. & KANE, C. L. 2010. Colloquium: topological insulators. *Reviews of Modern Physics,* 82**,** 3045.

HYBERTSEN, M. S. & LOUIE, S. G. 1986. Electron correlation in semiconductors and insulators: Band gaps and quasiparticle energies. *Physical Review B,* 34**,** 5390.

KIM, J., JANG, H., KOIRALA, N., SIM, S., LEE, J.-B., KIM, U. J., LEE, H., CHA, S., IN, C. & PARK, J. Gate-tunable, high-responsivity, and room-temperature infrared photodetectors based on a graphene-Bi 2 Se 3 heterostructure. Lasers and Electro-Optics (CLEO), 2016 Conference on, 2016. IEEE, 1-2.

KIM, J., PARK, S., JANG, H., KOIRALA, N., LEE, J.-B., KIM, U. J., LEE, H.-S., ROH, Y.-G., LEE, H. & SIM, S. 2017. Highly Sensitive, Gate-Tunable, Room-Temperature Mid-Infrared Photodetection Based on Graphene–Bi2Se3 Heterostructure. *ACS Photonics,* 4**,** 482-488.

KITTEL, C., MCEUEN, P. & MCEUEN, P. 1996. *Introduction to solid state physics*, Wiley New York.

LAWAL, A., SHAARI, A., AHMED, R. & JARKONI, N. 2017. First-principles many-body comparative study of Bi2Se3 crystal: A promising candidate for broadband photodetector. *Physics Letters A,* 381**,** 2993-2999.

LAWAL, A., SHAARI, A., AHMED, R. & TAURA, L. S. 2018. Investigation of excitonic states effects on optoelectronic properties of Sb2Se3 crystal for broadband photo-detector by highly accurate first-principles approach. *Current Applied Physics,* 18**,** 567-575.

LEE, J., KOO, J., CHI, C. & LEE, J. H. A harmonically mode-locked femtosecond fiber laser using bulk-structured Bi 2 Te 3 topological insulator. 2015 Conference on Lasers and Electro-Optics (CLEO), 2015. IEEE, 1-2.

LI, Z., CHEN, S., SUN, J., LI, X., QIU, H. & YANG, J. 2018. Spatial and thickness dependence of coupling interaction of surface states and influence on transport and optical properties of few-layer Bi2Se3. *Journal of Physics: Condensed Matter,* 30**,** 065503.

LIU, C.-X., ZHANG, H., YAN, B., QI, X.-L., FRAUENHEIM, T., DAI, X., FANG, Z. & ZHANG, S.-C. 2010. Oscillatory crossover from two-dimensional to three-dimensional topological insulators. *Physical review B,* 81**,** 041307.

LUCARINI, V., SAARINEN, J. J., PEIPONEN, K.-E. & VARTIAINEN, E. M. 2005. *Kramers-Kronig relations in optical materials research*, Springer Science & Business Media.

MAHDI, M. S., IBRAHIM, K., AHMED, N. M., HMOOD, A., MUSTAFA, F. I., AZZEZ, S. A. & BOUOUDINA, M. 2018. High performance and low-cost UV–Visible–NIR photodetector based on tin sulphide nanostructures. *Journal of Alloys and Compounds,* 735**,** 2256-2262.

MCIVER, J., HSIEH, D., DRAPCHO, S., TORCHINSKY, D., GARDNER, D., LEE, Y. & GEDIK, N. 2012. Theoretical and experimental study of second harmonic generation from the surface of the topological insulator Bi 2 Se 3. *Physical Review B,* 86**,** 035327.

PERDEW, J. P., BURKE, K. & ERNZERHOF, M. 1996. Generalized gradient approximation made simple. *Physical review letters,* 77**,** 3865.

POPOV, I., MANTEGA, M., NARAYAN, A. & SANVITO, S. 2014. Proximity-induced topological state in graphene. *Physical Review B,* 90**,** 035418.

QIAO, H., YUAN, J., XU, Z., CHEN, C., LIN, S., WANG, Y., SONG, J., LIU, Y., KHAN, Q. & HOH, H. Y. 2015. Broadband photodetectors based on graphene–Bi2Te3 heterostructure. *Acs Nano,* 9**,** 1886-1894.

RODRÍGUEZ-FORTUÑO, F. J., VAKIL, A. & ENGHETA, N. 2014. Electric levitation using ϵ-near-zero metamaterials. *Physical review letters,* 112**,** 033902.

SARKAR, S., YANG, J., TAN, L. Z., RAPPE, A. M. & KRONIK, L. 2018. Molecule-Adsorbed Topological Insulator and Metal Surfaces: A Comparative First-Principles Study. *Chemistry of Materials,* 30**,** 1849-1855.

SAVOIA, S., CASTALDI, G., GALDI, V., ALÙ, A. & ENGHETA, N. 2015. PT-symmetry-induced wave confinement and guiding in ε-near-zero metamaterials. *Physical Review B,* 91**,** 115114.

WANG, Z., MU, H., YUAN, J., ZHAO, C., BAO, Q. & ZHANG, H. 2017. Graphene-Bi 2 Te 3 Heterostructure as Broadband Saturable Absorber for Ultra-Short Pulse Generation in Er-Doped and Yb-Doped Fiber Lasers. *IEEE Journal of Selected Topics in Quantum Electronics,* 23**,** 1-5.

XIONG, Z., AN, X., LI, Z., XIAO, T. & CHEN, X. 2014. Phase transition, electronic, elastic and thermodynamic properties of Bi2Te3 under high pressure. *Journal of Alloys and Compounds,* 586**,** 392-398.

YAO, J., SHAO, J., WANG, Y., ZHAO, Z. & YANG, G. 2015. Ultra-broadband and high response of the Bi 2 Te 3–Si heterojunction and its application as a photodetector at room temperature in harsh working environments. *Nanoscale,* 7**,** 12535-12541.

YAZYEV, O. V., KIOUPAKIS, E., MOORE, J. E. & LOUIE, S. G. 2012. Quasiparticle effects in the bulk and surface-state bands of Bi 2 Se 3 and Bi 2 Te 3 topological insulators. *Physical Review B,* 85**,** 161101.

YAZYEV, O. V., MOORE, J. E. & LOUIE, S. G. 2010. Spin polarization and transport of surface states in the topological insulators Bi 2 Se 3 and Bi 2 Te 3 from first principles. *Physical review letters,* 105**,** 266806.

YUE, Z., WANG, X. & GU, M. 2018. Topological insulator materials for advanced optoelectronic devices. *arXiv preprint arXiv:1802.07841*.

ZHANG, H., LIU, C.-X., QI, X.-L., DAI, X., FANG, Z. & ZHANG, S.-C. 2009a. Topological insulators in Bi 2 Se 3, Bi 2 Te 3 and Sb 2 Te 3 with a single Dirac cone on the surface. *Nature physics,* 5**,** 438.

ZHANG, J., WANG, P., SUN, J. & JIN, Y. 2014. High-Efficiency Plasmon-Enhanced and Graphene-Supported Semiconductor/Metal Core–Satellite Hetero-Nanocrystal Photocatalysts for Visible-Light Dye Photodegradation and H2 Production from Water. *ACS applied materials & interfaces,* 6**,** 19905-19913.

ZHANG, Y. 2015. Communication: Surface stability and topological surface states of cleaved Bi2Se3: First-principles studies. AIP Publishing.

ZHANG, Y., HE, K., CHANG, C.-Z., SONG, C.-L., WANG, L., CHEN, X., JIA, J., FANG, Z., DAI, X. & SHAN, W.-Y. 2009b. Crossover of three-dimensional topological insulator of Bi2Se3 to the two-dimensional limit. *arXiv preprint arXiv:0911.3706*.